HHS Public Access

Author manuscript

Phys Med Biol. Author manuscript; available in PMC 2019 April 19.

Published in final edited form as:

Phys Med Biol. ; 63(8): 085016. doi:10.1088/1361-6560/aab532.

Quantitative assessment of cervical softening during pregnancy in the Rhesus macaque with shear wave elasticity imaging

Ivan M Rosado-Mendez[1,‡], **Lindsey C Carlson**[1], **Kaitlin M Woo**[2], **Andrew P Santoso**[1], **Quinton W Guerrero**[1], **Mark L Palmeri**[3], **Helen Feltovich**[4], and **Timothy J Hall**[1]

[1]Medical Physics Department, University of Wisconsin, Madison, WI, USA

[2]Biostatistics and Medical Informatics, University of Wisconsin, Madison, WI, USA

[3]Biomedical Engineering, Duke University, Durham, NC, USA

[4]Maternal Fetal Medicine, Intermountain Healthcare, Provo, UT, USA

Abstract

Abnormal parturition, e.g. pre- or post-term birth, is associated with maternal and neonatal morbidity and increased economic burden. This could potentially be prevented by accurate detection of abnormal softening of the uterine cervix. Shear Wave Elasticity Imaging (SWEI) techniques that quantify tissue softness, such as shear wave speed (SWS) measurement, are promising for evaluation of the cervix. Still, interpretation of results can be complicated by biological variability (i.e., spatial variations of cervix stiffness, parity), as well as by experimental factors (i.e., type of transducer, posture during scanning). Here we investigated the ability of SWEI to detect cervical softening, as well as sources of SWS variability that can affect this task, in the pregnant and nonpregnant Rhesus macaque. Specically, we evaluated SWS differences when imaging the cervix transabdominally with a typical linear array abdominal transducer, and transrectally with a prototype intracavitary linear array transducer. Linear mixed effects (LME) models were used to model SWS as a function of menstrual cycle day (in nonpregnant animals) and gestational age (in pregnant animals). Other variables included parity, shear wave direction, and cervix side (anterior vs. posterior). In the nonpregnant cervix, the LME model indicated that SWS increased by 2% (95% Confidence Interval 0-3%) per day, starting 8 days before menstruation. During pregnancy, SWS signicantly decreased at a rate of 6% (95% CI 5-7%) per week (intracavitary approach) and 3% (95% CI 2-4%) per week (transabdominal approach), and interactions between the scanning approach and other fixed effects were also significant. These results suggest that, while absolute SWS values are influenced by factors such as scanning approach and SWEI implementation, these sources of variability do not compromise the sensitivity of SWEI to cervical softening. Our results also highlight the importance of standardizing SWEI approaches to improve their accuracy for cervical assessment.

Keywords

Cervix; preterm birth; Shear Wave Elasticity Imaging; shear wave speed

‡Present address: Instituto de Fisica, Universidad Nacional Autonoma de Mexico, Mexico City, MEX

1. Introduction

Irrespective of when birth occurs, the cervix is the gatekeeper to delivery. During pregnancy, the uterine cervix undergoes a remarkable structural transformation from a stiff enclosure into a compliant and effaced opening to allow for vaginal delivery.(Timmons, Reese, Socrate, Ehinger, Paria, Milne, Akin, Auchus, McIntire, House & Mahendroo 2014) Normal parturition (pregnancy and delivery) involves precise timing of this process. Pre- or post-term delivery, however, is associated with important adverse outcomes. For instance, spontaneous preterm birth (sPTB) is the primary global cause of death in children under 5 years old, and can lead to lifelong health complications in those that survive.(Chang, Larson, Blencowe, Spong, Howson, Cairns-Smith, Lackritz, Lee, Mason, Serazin, Walani, Simpson & Lawn 2013, Feltovich, Hall & Berghella 2012) On the other end of the spectrum, post-term pregnancy can result in stillbirth, or complications from failed induction of labor in an attempt to prevent stillbirth. (Gülmezoglu, Crowther, Middleton & Heatley 2012, Rouse, Weiner, Bloom, Varner, Spong, Ramin, Caritis, Grobman, Sorokin, Sciscione, Carpenter, Mercer, Thorp, Malone, Harper, Iams & Anderson 2011, Spong, Berghella, Wenstrom, Mercer & Saade 2012) Poor outcomes resulting from pre- or post-term delivery could potentially be prevented by accurate detection of abnormal cervical change. However, current understanding of the intricate synchrony of physiological processes involved in parturition is limited. The possibility of detecting early softening that precedes sPTB, or delayed softening that results in post-term pregnancy, has motivated numerous research efforts to describe changes in morphological and mechanical properties of the cervix during pregnancy.

Evaluation of morphological features is most often done with transvaginal ultrasound, which allows measurement of cervical length and observation of funneling of the internal os (the junction of the proximal cervix and uterus where cervical change initiates). Clinical assessment of the mechanical properties of the cervix (i.e., its softness) is routinely done by subjective digital palpation. Unsurprisingly, prediction of delivery timing (at either end of the parturition spectrum) is notoriously poor.(Feltovich 2017, Swiatkowska-Freund & Preis 2017) Therefore, there is a need for objective and specific methods to identify cervical properties associated with abnormal parturition. Ultrasound-based Shear Wave Elasticity Imaging (SWEI) has been proposed for this task.(Carlson, Feltovich, Palmeri, del Rio & Hall 2014, Muller, Aït-Belkacem, Hessabi, Gennisson, Grangé, Goffinet, Lecarpentier, Cabrol, Tanter & Tsatsaris 2015, Peralta, Rus, Bochud & Molina 2015, Rosado-Mendez, Palmeri, Drehfal, Guerrero, Simmons, Feltovich & Hall 2017)

SWEI allows for non-invasive quantification of parameters related to tissue stiffness, such as shear wave speed (SWS), by analyzing the propagation of shear waves induced by acoustic radiation force impulse (ARFI) excitations.(Nightingale 2011, Sarvazyan, Hall, Urban, Fatemi, Aglyamov & Garra 2011) The mechanical response of the cervix to ARFI stimuli is defined by the structural components of its extracellular matrix.(Myers, Paskaleva, House & Socrate 2008, Kuo, Charng, Wu & Li 2017) These include bundles of collagen arranged in layers longitudinal or concentric to the cervical canal, as well as other components such as proteoglycans and elastin which inform viscoelastic properties. (House & Socrate 2006, Reusch, Feltovich, Carlson, Hall, Campagnola, Eliceiri & Hall 2013, Yao, Gan, Myers,

Vink, Wapner & Hendon 2016) We and others (Peralta, Rus, Bochud & Molina 2015, Carlson, Feltovich, Palmeri, Dahl, del Rio & Hall 2014, Huang, Drehfal, Rosado-Mendez, Guerrero, Palmeri, Simmons, Feltovich & Hall 2016, Muller et al. 2015) have demonstrated that, although this complex structure complicates shear wave propagation and forbids the derivation of inherent mechanical tissue properties (such as Young's modulus E or the shear modulus μ) from SWS estimates, the latter can be potentially used as a biomarker to track spatial and temporal gradients in cervical stiffness.

The value of a biomarker as a surrogate endpoint for cervical softening relies on its potential to objectively quantify softening.(Aronson 2005) Translating experimental SWEI to routine cervical assessment during pregnancy can be complicated by sources of SWS variability other than those associated with cervical softening. These sources of variability can be due to biological or experimental factors. Biological factors can include differences in stiffness between the anterior and posterior portions of the cervix, as well as between subjects with or without previous pregnancies, i.e., parity. Examples of experimental factors are the use of transducers with different frequency ranges and focal configurations, as well as variation in posture during scanning (which affects mechanical load on the cervix). All these factors can reduce the sensitivity of SWEI to cervical softening and confound the interpretation of SWS changes.

Animal models can help clarify the conditions under which SWS can be used for cervical assessment.(Peralta, Mourier, Richard, Charpigny, Larcher, Aït-Belkacem, Balla, Brasselet, Tanter, Muller & Chavatte-Palmer 2015, Huang et al. 2016) Nonhuman primates (NHP) such as Rhesus macaques share similarities with humans regarding maternal-fetal immunology and physiology, monthly menstrual cycles, singleton pregnancies, mechanical loading (non-obligated quadripeds), and pregnancy complications.(Haluska, West, Novy & Brenner 1990, Hafez & Jaszczak 1972, Owiti, Tarantal, Lasley & Hendrickx 1989, Wolfgan, Eisele, Knowles, Browne, Schotzko & Golos 2001, Adams-Waldorf, Singh, Mohan, Young, Ngo, Das, Tsai, Bansal, Paolella, Herbert, Sooranna, Gough, Astley, Vogel, Baldessari, Bammler, MacDonald, Gravett, Rajagopal & Johnson 2015) With an NHP model, under highly-controlled experiments with *ex vivo* tissue, SWS estimation has been shown to be sensitive to changes in spatial gradients of cervical softness induced with misoprostol, a prostaglandin commonly used for induction of labor in women.(Huang et al. 2016, Rosado-Mendez et al. 2017) Thus, the Rhesus holds promise as a suitable NHP model for understanding cervical softening and parturition.

This work investigates whether SWEI can objectively detect gradual changes in cervical softness *in vivo* in Rhesus macaques. In particular, we evaluate the effects of experimental and biological sources of variability. To this end we compared SWS measurements from two experimental approaches: imaging the cervix with a transabdominal approach (TA) and an intracavitary approach (IC). Each approach makes use of a suitable transducer: a conventional abdominal linear array for the TA approach, and a prototype catheter transducer for the IC approach. We also investigated biological factors including effects of the menstrual cycle in the nonpregnant cervix, cervix side and parity. We demonstrate that, although absolute values of SWS are influenced by the menstrual status (indicating softening in the days prior to menses as expected from hormonal influence), cervix side and scanning

approach, both SWEI approaches are sensitive to cervical softening during pregnancy. We also demonstrate that, to further advance the translation of SWEI-based cervical assessment to the clinic, future work needs to focus on its standardization to improve its reliability.

2. Materials and Methods

The study was divided in two parts: the “pre-pregnancy” stage, and the “pregnancy” stage. The goal of the pre-pregnancy stage was to elucidate factors affecting SWS quantification in the nonpregnant cervix. The pregnancy stage assessed the feasibility of objectively tracking changes in cervical softness during pregnancy with SWS. The protocol was approved by the University of Wisconsin Institutional Animal Care and Use Committee and was performed in accordance with federal guidelines of proper animal care.

2.1. Data Acquisition

For the pre-pregnancy stage, 10 non-pregnant Rhesus (5 nulliparous, 5 multiparous) were recruited from the Wisconsin National Primate Research Center (WNPRC). Each subject was scanned eight times during 2 consecutive (approx. 28-day) menstrual cycles. The pregnancy stage included 18 primates (10 nulliparous, 8 multiparous), 8 of which came from the pre-pregnancy stage (the other 2 of these animals did not achieve pregnancy after breeding). Subjects were scanned at weeks 4, 10, 16, 20, and 23 during the 25-week long gestation. Median [range] age and weight of these subjects are summarized in table 1.

In both stages, the subject was anesthetized with 10 to 20 mg of ketamine per kilogram of body weight five minutes prior to the procedure. Scanning sessions occurred in an operating room at the WNPRC where the subject was closely monitored by an WNPRC research specialist (M.S.). Each procedure started by placing the subject on her back. Her lower abdomen was shaved (for acoustic coupling). Data acquisition was performed by a sonographer and staff trained by a Maternal Fetal Medicine specialist physician (H.F.) to identify anatomical landmarks such as the anterior and posterior cervix, the internal os (uterine end of the cervix), the external os (vaginal end of the cervix), the cervical canal, the uterus, and the bladder. First, SWEI was applied to the cervix transabdominally with a 38 mm field-of-view linear array (9L4) transducer on a Siemens Acuson S2000 ultrasound scanner (Siemens Healthcare, Ultrasound Business Unit, Mountain View, CA, USA). After transabdominal SWEI, the subject was positioned to rest on her left side for transrectal SWEI. A prototype catheter transducer (128 elements, 14 mm aperture, 3 mm diameter) was fixed to the user's index finger with a Tegaderm™ film (to minimize motion of the transducer and to reduce pre-loading by minimizing contact force on the cervix) and then covered with a gel-filled glove. The transducer was inserted in the rectal cavity (rectal exam is standard for evaluating the cervix in macaques) and placed over the posterior cervix. Figure 1 shows diagrams of the data acquisition of each approach, as well as B-mode images with key anatomical features. Because of limited acoustic output of the catheter transducer and the stiff non-pregnant NHP cervix,(Huang et al. 2016, Rosado-Mendez et al. 2017) the intracavitary approach was used only on the pregnant cervix.

In both scanning approaches, SWEI data were acquired via a customized implementation of the Siemens Virtual Touch Tissue Quantification software package. Shear waves were

created with an ARFI technique(Nightingale 2011) and tracked within a 6×5mm^2 region of interest (ROI) placed at the mid-proximal location (near the uterine end of the cervix; white box in B-mode images of figure 1). Previous studies in humans and NHPs showed structural similarities between the human and NHP cervix at this location, as well as reliable SWS estimation and sensitivity to exogenous ripening.(Huang et al. 2016, Rosado-Mendez et al. 2017) In the transabdominal (TA) approach, the ROI was repositioned between 4 to 6 times on both the anterior and posterior halves of the cervix. In the transrectal (intracavity; IC) approach, one SWEI acquisition was performed in each cervix side. At each ROI position, five SWEI acquisitions were performed. Each acquisition tracked the propagation of two opposing waves propagating from the internal to the external os (I2E) and from the external to the internal os (E2I) to test directionality of SWS estimates. Pushing and tracking parameters for the two scanning approaches are shown in table 2.

2.2. Data processing

In-phase and quadrature data from tracking frames were obtained from the scanner's Axius Direct User Research Interface (Brunke, Insana, Dahl, Hansen, Ashfaq & Ermert 2007) and processed offline in MATLAB (Mathworks, Natick, MA, USA) using custom-built routines. Shear-wave induced displacements were estimated with Loupas' correlation method. (Loupas, Gill & Peterson 1995) Displacement estimates with a correlation coefficient <0.98 were discarded. Low-frequency biological motion was removed with a second-order polynomial motion filter.(Nightingale, Rouze, Rosenzweig, Wang, Abdelmalek, Guy & Palmeri 2015) Filtered displacements from the 5 ARFI data sets for each wave direction at one ROI location were averaged to reduce noise. Due to the limited acoustic output, displacements obtained from the catheter transducer were low-passed filtered at 1.5kHz. The presence of tissue layers within the ROI was determined by locating axial discontinuities in the time-averaged displacement field, as described in our previous *ex vivo* study.(Rosado-Mendez et al. 2017) If layers were detected, SWS were obtained from each layer separately.

SWS was estimated from tissue displacements using a RANdom SAmple Consensus (RANSAC) algorithm.(Wang, Palmeri, Rotemberg, Rouze & Nightingale 2010) This technique fits a plane to the “time-of-flight” (TOF) of peak displacements as a function of depth and lateral distance from the ARFI excitation. To assess the quality of SWS estimates, we followed a strategy proposed in our previous *ex vivo* study(Rosado-Mendez et al. 2017) which combines a metric of goodness of fit of the RANSAC estimator (the fraction of TOF points lying on the fitted plane) and a metric of reliability by comparing SWS RANSAC estimates to estimates from the Radon Sum estimator (a different TOF method based on maximizing trajectories of integrated displacements in the “time-vs.-distance” plane). (Rouze, Wang, Palmeri & Nightingale 2010) SWS estimates with less than 50% inliers and/or a disagreement in SWS greater than 2.5 m/s between the two SWS estimation methods were discarded. SWS estimates in the TA approach from repeated SWEI acquisitions in which the ROI was repositioned 4-6 times in the same cervix side were combined in a weighted-average. Each SWS value was weighted by a Quality Index defined by the ratio of the percentage of TOF inliers and the absolute difference of the RANSAC and Radon Sum SWS values.

2.3. Analysis of SWS in the non-pregnant cervix

First, we investigated biological and experimental factors affecting SWS estimates in the non-pregnant Rhesus macaque cervix. A linear mixed effects (LME) model was used to estimate the relationship between SWS and menstrual cycle day (continuous variable 'Day'), cervix side (anterior/posterior, categorical predictor 'Side'), wave direction (I2E/E2I, categorical predictor 'Dir'), and parity (nulliparous/multiparous, categorical predictor 'Par') fitted using maximum likelihood. In a preliminary assessment of the variation of SWS during the menstrual cycle,(Rosado-Mendez et al. 2016) we observed that the lowest values occurred 8 days before menstruation, and increased after menstruation. Thus, to approximate a monotonically increasing variation, we defined Day 0 as 8 days before menstruation for each subject. Uncorrelated random effects due to inter-subject and inter-cycle variability for slope and intercept were included. A natural logarithmic transformation was applied to SWS to satisfy the normality assumption of the analysis. The LME model can be represented as follows:

$$log\ (\mathrm{SWS}) = a' + b' * \mathrm{Day} + c * \mathrm{Side} + d * \mathrm{Dir} + e * \mathrm{Par} \quad (1)$$

where $'$ variables include random effects. From this model, 95% confidence intervals were estimated for the fixed effects via parametric bootstrapping (10,000 iterations), and approximate p values were subsequently found via inversion of estimated confidence intervals. Statistical analysis was performed in R 3.3.1,(R Core Team 2013) including the 'lme4' package.(Galecki & Burzykowski 2013)

We also investigated other possible experimental factors associated with the TA approach regarding the control of the orientation of the cervix with respect to the transducer. For example, figure 2 shows B-mode images of two examples in which the cervix is at a 4.0° angle (a) and a 41.6° angle (b) with respect to the face of the transducer. Furthermore, the supine position caused the bladder to be above the cervix. In many cases, the bladder was partially full. To determine the influence of these sources of variability in the analysis, we studied the relationship between SWS estimates made in the nonpregnant NHP cervix with (i) the angle between the cervical canal and the transducer and (ii) the thickness of the bladder region immediately above the SWS-tracking ROI. The correlations of angle between the cervical canal and the transducer and bladder thickness (mm) with SWS were analyzed using Spearman's rank correlation.

Another possible confounder was the use of a gel-based standoff pad between the transducer and the animal's skin to allow optimal focusing with the transabdominal transducer in cases where the cervix was very shallow. An example of the use of the standoff pad is shown in figure 2(a). SWS values in the nonpregnant cervix were compared between using versus not using the standoff pad by means of the Wilcoxon rank sum test.

2.4. Analysis of SWS in the pregnant cervix

Second, we investigated whether the TA and IC approaches provide SWS estimates that can be used as objective biomarkers of cervical softening during pregnancy. To this end, a

maximum-likelihood linear mixed effects model was fit to SWS versus gestational age to compare the change in SWS during pregnancy between the two experimental approaches. Fixed effects included gestational age in weeks after conception (continuous predictor 'GA'), scanning approach (TA/IC, categorical predictor 'App'), cervix side, wave direction, and parity. A natural logarithmic transformation was applied to SWS to satisfy the normality assumption of the analysis. The model can be represented as:

$$log\ (\mathrm{SWS}) = h' + j' * \mathrm{GA} + k * \mathrm{App} + l * \mathrm{Side} + m * \mathrm{Dir} + n * \mathrm{Par} + \cdots \quad (2)$$

Inter-subject variability was accounted for as a random effect for intercept and slope. To account for possible dependence of the influence of fixed effects on the scanning approach, interactions between App and the other fixed effects were included. To this end, the following terms were also included in (2):

$$\cdots + o * \mathrm{App} * \mathrm{GA} + p * \mathrm{App} * \mathrm{Side} + q * \mathrm{App} * \mathrm{Dir} + r * \mathrm{App} * \mathrm{Par}\,. \quad (3)$$

3. Results

3.1. Analysis of SWS in the non-pregnant cervix

The duration of menstrual cycle varied among subjects and within subjects. The median [range] of the menstrual cycle duration was 27.5 days [22-43 days]. The median [range] of the difference in duration of two consecutive menstrual cycles of one subject was 1 day [0-4 days].

SWS in the nonpregnant cervix was found to be mainly influenced by the cervix side and menstrual cycle status. This is indicated by the p values of the LME model (table 3) of these descriptors, which were 10 times smaller than those of parity ($p = 0.41$) and wave direction ($p = 0.58$). SWS values were found to be larger in the posterior side than in the anterior side by a factor of $c = 1.28$ (95% CI 1.05-1.55). The LME model indicates a trend toward SWS increases after Day 0 by a factor of $b' = 1.02$ (or a 2% increment) per day (95% CI 1.00-1.03) with respect to the base value given by the intercept ($SWS_0 = a' = 2.56$m/s, 95% CI 1.67-3.89m/s).

Figure 3 shows the log-transformed SWS as a function of the day within the menstrual cycle in (a) the anterior and (b) posterior cervix. Because the exact day of measurement with respect to Day 0 varied between consecutive cycles of a subject and among subjects, data points were grouped into three 8-9 day periods, as done in the preliminary assessment, for better visualization.(Rosado-Mendez et al. 2016) To avoid possible bias in the assessment of SWS changes within the menstrual cycle imposed by the linear model, we also compared average SWS values among the three 8-9 day periods by means of a Kruskal-Wallis non-parametric test of statistical significance. We found a significant increase ($p = 0.04$) of SWS in the third period (approximately 12 days before menstruation) in the posterior cervix.

Figures 4(a) and (b) show scatter plots of the RANSAC SWS estimates vs. the cervix angle and the bladder thickness. Spearman's correlations were weak (ρ(SWS vs. angle)=-0.157 and ρ(SWS vs bladder thickness)=-0.264) and not significant.

Figure 5 shows boxplots of all RANSAC SWS estimates made in the nonpregnant cervix with and without a standoff pad. When using the standoff pad, SWS estimates were significantly larger ($p < 0.001$) than when not using it.

3.2. Analysis of SWS in the pregnant cervix

The length of pregnancy ranged between 23.3 and 25.6 weeks among subjects, representing only about 1 week or 4.7% about the median (24.6 weeks).

The LME model of the pregnant cervix (table 4) indicated that SWS was mainly defined by gestational age, scanning approach and cervix side (these predictors with $p \leq 0.0001$), and to a lesser extent by wave direction ($p = 0.014$). Figure 6 shows the log-transformed SWS as a function of the weeks of gestation. Subfigures (a) and (b) on the top row correspond to the TA approach in the anterior and posterior sides, respectively, and (c) and (d) on the bottom row to the IC approach in the corresponding sides. The LME model indicated that SWS for the IC approach significantly decreased by a factor of $j = 0.94$ per week (95% CI 0.93-0.95), or a decline of 6%, per week. Smaller SWS values were observed with the TA approach than with the IC approach (by a factor of $k = 0.78$ (95% CI 0.70-0.86)), in the posterior side than in the anterior side (by a factor of $l = 0.93$ (95% CI 0.89-0.96)), and with waves moving in the E2I direction than in the I2E direction (by a factor of $m = 0.96$ (95% CI 0.92-0.99)).

Significant interactions were observed between the TA approach and gestational age, cervix side and wave direction. The interaction between App and gestational age ($p < 0.0001$) indicated that for the TA approach, SWS decreased by a factor of $j^*o = 0.94^*1.03 = 0.97$ (95% CI 0.96-0.98), or a decline of 3%, per week. The interaction of App with cervix side and wave direction indicated that the difference between anterior and posterior sides is larger with the TA approach ($l^* p = 0.93 * 0.82 = 0.76$), while the effect of wave direction is inverted ($m^* q = 0.95 * 1.13 = 1.09$).

4. Discussion

In the nonpregnant cervix, the LME model indicated modest influence ($p = 0.07$) of the menstrual status on SWS (table 3). This was supported by the lack of statistical significance of SWS differences among periods of the menstrual cycle (only one difference had $p < 0.05$ in the posterior cervix) (figure 3). In spite of the limited significance (probably attributable to data paucity and high SWS variance), our results suggest a trend toward SWS variation by day of menstrual cycle of the Rhesus, with slower SWS, indicating softer tissue, during the luteal phase prior to menses. This is consistent with other mammals. For example, Harkness et al.(Harkness & Harkness 1959) reported that in rats, the cervix is stiffer at the onset of the estrus phase (during which ovulation occurs, characterized by high levels of estrogen) than at the onset of the diestrus phase (in which the corpus luteum matures, with rising levels of progesterone). In women, the menstrual cycle is divided in three phases: the menstrual phase (approx. 5 days, during which menses occurs), the follicular phase (approx. 8 days,

involving follicle development and ovulation, characterized by high levels of estrogen), and the luteal phase (approx. 13 days, between ovulation and the next menses, dominated by progesterone).(Heitz et al. 1999) The cycle of the Rhesus macaque is similar.(Gilardi, Shideler, Valverde, Roberts & Lasley 1997) We are interested in these hormonal changes because they directly influence reproductive tissue properties. For example, estrogen is associated with a reduction in collagen synthesis and an increase in collagen degradation, which results in a decrease in the diameter and density of collagen fibers, and leads to softer tissue.(Hama, Yamamuro & Takeda 1976, Kjær & Hansen 2008, Li, Wang, Fan, Kang, Liu, Zhang & Wang 2015) Similar changes have been observed in nonpregnant women via Raman spectroscopy.(Kanter, Majumder, Kanter, Woeste & Mahadevan-Jansen 2009, Kanter, Vargis, Majumder, Keller, Woeste, Rao & Mahadevan-Jansen 2009) Further, elevated intracervical progesterone levels in pregnant women appear to stabilize cervical change until cervical remodeling becomes rapid near delivery. Given this, one would expect the follicular phase in both women and Rhesus to be associated with changes to cervical collagen that manifest in softening during the luteal phase, followed by menses (unless pregnancy occurs, in which case progesterone and estrogen both sharply increase and the cervix continues to soften). In summary, our results suggest cervical softening in the days prior to menses, which is both biologically plausible and consistent with previous observations in women.

The only significant SWS predictor (source of difference among measurements) in the nonpregnant cervix was cervix side, i.e., anterior vs. posterior. This finding is consistent with our previous studies in the *ex vivo* human and Rhesus cervix.(Rosado-Mendez et al. 2017) It is also consistent with recent findings from a study using optical coherence tomography to quantify collagen fiber alignment in cross-sectional slices of the proximal cervix. Yao et al.(2016) found that the anterior and posterior quadrants have highly aligned collagen fibers that circle around the cervical canal, with posterior fibers showing slightly more alignment than anterior ones. Because stiffness of highly anisotropic collagenous materials depends on the degree of collagen fiber alignment,(Namani, Wood, Sakiyama-Elbert & Bayly 2009) it is possible that differences in fiber alignment between anterior and posterior sides, in addition to different anatomical stresses on each cervix side, might have contributed to observed differences in SWS and its changes during the menstrual cycle in nonpregnant macaques.

We also found that the use of a standoff pad (in the transabdominal approach) had a significant effect on SWS values (figure 5). This can be attributed to the lower attenuation that the ARFI excitation experiences when using the standoff pad compared to the attenuation of intervening tissues, resulting in shear waves with higher frequency content and thus larger SWS values. To test the influence of the use of the standoff pad on the rate of SWS change during the menstrual cycle and pregnancy, an interaction was added to each LME model between a binary variable that considered the use (or not) of the standoff pad with the predictors ‘Day’ and ‘GA’. The interactions were not significant. Thus, the use of the standoff pad did not significantly influence the rates of SWS change during the menstrual cycle or during pregnancy.

SWS was found to significantly decrease with pregnancy regardless of the scanning approach. Rates of SWS reduction were 6% per week with the IC approach, and 3% with the TA approach. Over the 24-25 weeks of pregnancy, these rates resulted in a total reduction of 78% and 53% of the non-pregnant cervix SWS value. In a recent cross sectional study in pregnant humans, we observed a reduction in SWS of 52% between the first and third trimester cervix.(Drehfal, Hall, Rosado-Mendez, Palmeri & Feltovich 2017) These reductions are similar to those reported by Peralta et al. (2015) when inducing cervical ripening in pregnant ewes (54%) and larger than the ones reported by Muller et al. (2015) in humans (12%, probably due to their assessment of the distal cervix instead of the mid-proximal). The larger SWS reduction observed in primates can be attributed to the stiffer nature of the non-pregnant Rhesus cervix compared to women. Recently, we observed a significant SWS reduction of 26% in the anterior side of the *ex vivo*, non-pregnant Rhesus cervix after exogenous ripening induction with misoprostol (Rosado-Mendez et al. 2017) analogous to that observed in *ex vivo* humans. (Carlson, Feltovich, Palmeri, del Rio & Hall 2014)

In addition to significant differences in the rate of SWS reduction between approaches, significant interactions were observed between the scanning approach and gestational age, cervix side and wave direction. Taken together, these results suggest that the interplay between changes in cervical structural and chemical properties during pregnancy with the different mechanical loads inherent to each scanning approach influence the sensitivity of SWEI to cervical softening. The complexity of the anatomical forces acting on the cervix in each position makes it very difficult to infer these interactions. This knowledge could be achieved through computational models, such as the finite element model designed by Fernandez et al. (2016) for the human cervix.

Figures 5 and 6 show large variability in SWS values in the nonpregnant and the pregnant cervix, particularly when compared to values from liver tissue where SWEI has been widely investigated.(Nightingale et al. 2015, Palmeri, Wang, Dahl, Frinkley & Nightingale 2008, Palmeri et al. 2008, Ferraioli, Filice, Castera, Choi, Sporea, Wilson, Cosgrove, Dietrich, Amy, Bamber et al. 2015) This variability can be attributed to the larger stiffness of the macaque cervix compared to liver (SWS between 1 and 1.7m/s). In homogeneous elastic solids, the standard deviation of SWS estimates from time-of-flight methods increases with the square of the shear wave speed.(Wang, Byram, Palmeri, Rouze & Nightingale 2013) Moreover, the cervix is a structurally complex and viscoelastic medium.(Reusch et al. 2013, Huang et al. 2016, Rosado-Mendez et al. 2017) The spatial heterogeneity of the cervix collagen structure increases SWS intra- and inter-subject variability because of slight variations of ROI positioning with respect to the cervix structure. In addition, variation in the shear wave frequency content (due, for example, to different degrees of acoustic attenuation caused by intervening tissues between the transducer and the ROI) can lead to higher sensitivity to shear wave dispersion (dependence of shear wave speed on frequency), which has been shown to be large in the Rhesus macaque cervix compared to other tissues. (Rosado-Mendez et al. 2017)Notwithstanding these sources of variance, our results demonstrate that sensitivity of SWEI to cervical softening during pregnancy was not compromised with either of the scanning approaches.

In summary, this study demonstrates the sensitivity of SWS to cervical softening (both during the menstrual cycle and during pregnancy), as well as to other biological and experimental factors that must be considered when interpreting SWS values. In other words, although SWEI clearly has merit for evaluating cervical softening, on an absolute scale, SWS depends strongly on the experimental technique. Therefore, to advance the translation of SWEI as a routine clinical tool for cervical assessment, efforts should be focused on standardizing the technique and identifying other possible factors that may compromise the distinction of abnormal from normal cervical softening. Future studies will delve into the correlation between the biochemical subtleties of parturition and the mechanical properties of the cervix.

Current clinical ability to predict timing of delivery is extremely poor, in part because fundamental parturiton is incompletely understood. As the gatekeeper to delivery, the cervix is a primary focus of clinicians; both the American College of Obstetricians and Gynecologists and the Society for Maternal-Fetal medicine recommend midtrimester transvaginal ultrasound cervical length screening for prediction of preterm birth because a short cervix is inversely correlated with gestational age at delivery. (Iams, Goldenberg, Meis, Mercer, Moawad, Das, Thom, McNellis, Copper, Johnson et al. 1996) However, although cervical length measurement is currently the best that obstetrics has to offer, it is highly unspecific; in the original study, and hundreds of subsequent studies, it has been demonstrated that most women with a short cervix in the midtrimester deliver at term, and most women with preterm delivery have a normal midtrimester cervical length.(Feltovich 2017) The addition of objective measures of tissue properties such as softening to evaluation of the cervix has promise for enhancing understanding of the parturition process, and therefore many recent efforts to objectively assess the cervix focus on this characteristic. Although further investigation, including standardization of SWEI, is necessary, our results suggest that this technique has potential as a noninvasive biomarker of cervical compliance during pregnancy. Comprehensive understanding of the parturition process is the first step toward addressing problems related to abnormal timing of delivery, such as pre- or post-term birth.

5. Conclusion

SWS was found to change in the non-pregnant Rhesus macaque during the menstrual cycle, suggesting the high sensitivity SWEI to the small changes in cervical stiffness compared to those occurring during pregnancy. SWEI showed significant reductions of the SWS vs gestational age with both transabdominal and intracavitary approaches, thus confirming that SWEI is useful to track relative changes in the stiffness of the cervix during pregnancy. However, we observed significant differences between the approaches, indicating that, on an absolute scale, changes in SWS depend on scanning technique and data acquisition. Therefore, standardization of SWEI methodologies is needed to advance the clinical use of SWS as a biomarker for cervical softening.

Acknowledgments

The authors would like to thank Sarah Kohn and Michele Shotzko for their invaluable help in the data acquisition, as well as to Siemens Ultrasound for lending the scanner and technical support. This work was supported by NIH

grants T32CA009206 from the National Cancer Institute, and F31HD082911, R21HD061896, R21HD063031, and R01HD072077 from the Eunice Kennedy Shriver National Institute of Child Health and Human Development. We also thank the Instituto de Fisica of the Universidad Nacional Autonoma de Mexico for financial support (I.R-M.). The content is solely the responsibility of the authors and does not necessarily represent the official views of the National Institutes of Health.

References

Adams-Waldorf KM, Singh N, Mohan AR, Young RC, Ngo L, Das A, Tsai J, Bansal A, Paolella L, Herbert BR, Sooranna SR, Gough GM, Astley C, Vogel K, Baldessari AE, Bammler TK, MacDonald J, Gravett MG, Rajagopal L, Johnson MR. Uterine overdistention induces preterm labor mediated by inflammation: observations in pregnant women and nonhuman primates. American Journal of Obstetrics and Gynecology. 2015; 213(6):1–19. [PubMed: 26113225]

Aronson JK. Biomarkers and surrogate endpoints. British Journal of Clinical Pharmacology. 2005; 59(5):491–494. [PubMed: 15842546]

Brunke SS, Insana MF, Dahl JJ, Hansen C, Ashfaq M, Ermert H. An ultrasound research interface for a clinical system. IEEE Transactions on Ultrasonics, Ferroelectrics, and Frequency Control. 2007; 54(1):198–210.

Carlson LC, Feltovich H, Palmeri ML, Dahl J, del Rio AM, Hall TJ. Estimation of shear wave speed in the human uterine cervix. Ultrasound in Obstetrics & Gynecology. 2014; 43(4):452–458. [PubMed: 23836486]

Carlson LC, Feltovich H, Palmeri ML, del Rio AM, Hall TJ. Statistical analysis of shear wave speed in the uterine cervix. IEEE Transactions on Ultrasonics, Ferroelectrics, and Frequency Control. 2014; 61(10):1651–1660.

Chang HH, Larson J, Blencowe H, Spong CY, Howson CP, Cairns-Smith S, Lackritz EM, Lee SK, Mason E, Serazin AC, Walani S, Simpson JL, Lawn JE. Preventing preterm births: analysis of trends and potential reductions with interventions in 39 countries with very high human development index. The Lancet. 2013; 381(9862):223–234.

Drehfal LC, Hall TJ, Rosado-Mendez IM, Palmeri ML, Feltovich H. Detection of changes in cervical softness using shear wave speed in early vs. late pregnancy: an initial in vivo application. Ultrasound in Medicine & Biology Accepted. 2017

Feltovich H. Cervical evaluation. Obstetrics & Gynecology. 2017; 130(1):51–63. [PubMed: 28594774]

Feltovich H, Hall TJ, Berghella V. Beyond cervical length: emerging technologies for assessing the pregnant cervix. American Journal of Obstetrics and Gynecology. 2012; 207(5):345–354. [PubMed: 22717270]

Fernandez M, House M, Jambawalikar S, Zork N, Vink J, Wapner R, Myers K. Investigating the mechanical function of the cervix during pregnancy using finite element models derived from high-resolution 3d mri. Computer Methods in Biomechanics and Biomedical Engineering. 2016; 19(4):404–417. [PubMed: 25970655]

Ferraioli G, Filice C, Castera L, Choi BI, Sporea I, Wilson SR, Cosgrove D, Dietrich CF, Amy D, Bamber JC, et al. Wfumb guidelines and recommendations for clinical use of ultrasound elastography: Part 3: liver. Ultrasound in Medicine and Biology. 2015; 41(5):1161–1179. [PubMed: 25800942]

Gałecki, A., Burzykowski, T. Linear mixed-effects model. In: Gałecki, A., Burzykowski, T., editors. Linear Mixed-Effects Models Using R. Springer; New York, NY: 2013. p. 245-273.

Gilardi KVK, Shideler SE, Valverde CR, Roberts JA, Lasley BL. Characterization of the onset of menopause in the rhesus macaque. Biology of Reproduction. 1997; 57:335–340. [PubMed: 9241047]

Gülmezoglu, AM., Crowther, CA., Middleton, P., Heatley, E. Induction of labour for improving birth outcomes for women at or beyond term. In: Gülmezoglu, AM., editor. Cochrane Database of Systematic Reviews. John Wiley & Sons, Ltd; Chichester, UK: 2012.

Hafez ESE, Jaszczak S. Comparative anatomy and histology of the cervix uteri in non-human primates. Primates. 1972; 13(3):297–314.

Haluska GJ, West NB, Novy MJ, Brenner RM. Uterine estrogen receptors are increased by ru486 in late pregnant rhesus macaques but not after spontaneous labor. The Journal of Clinical Endocrinology & Metabolism. 1990; 70(1):181–186. [PubMed: 2294130]

Hama H, Yamamuro T, Takeda T. Experimental studies on connective tissue of the capsular ligament: Influences of aging and sex hormones. Acta Orthopaedica Scandinavica. 1976; 47(5):473–479. [PubMed: 998180]

Harkness MLR, Harkness RD. Changes in the physical properties of the uterine cervix of the rat during pregnancy. Journal of Physiology. 1959; 148:524–547. [PubMed: 14399825]

Heitz NA, Eisenman PA, Beck CL, Walker JA. Hormonal changes throughout the menstrual cycle and increased anterior cruciate ligament laxity in females. Journal of Athletic Training. 1999; 34(2): 144–149. [PubMed: 16558557]

House M, Socrate S. The cervix as a biomechanical structure. Ultrasound in Obstetrics & Gynecology. 2006; 28(6):745–749. [PubMed: 17063451]

Huang B, Drehfal LC, Rosado-Mendez IM, Guerrero QW, Palmeri ML, Simmons HA, Feltovich H, Hall TJ. Estimation of shear wave speed in the rhesus macaques uterine cervix. IEEE Transactions on Ultrasonics, Ferroelectrics, and Frequency Control. 2016; 63(9):1243–1252.

Iams JD, Goldenberg RL, Meis PJ, Mercer BM, Moawad A, Das A, Thom E, McNellis D, Copper RL, Johnson F, et al. The length of the cervix and the risk of spontaneous premature delivery. New England Journal of Medicine. 1996; 334(9):567–573. [PubMed: 8569824]

Kanter EM, Majumder S, Kanter GJ, Woeste EM, Mahadevan-Jansen A. Effect of hormonal variation on raman spectra for cervical disease detection. American Journal of Obstetrics and Gynecology. 2009; 200(5):512.e1–12.e5. [PubMed: 19236872]

Kanter EM, Vargis E, Majumder S, Keller MD, Woeste E, Rao GG, Mahadevan-Jansen A. Application of raman spectroscopy for cervical dysplasia diagnosis. Journal of Biophotonics. 2009; 2(1-2):81–90. [PubMed: 19343687]

Kjær M, Hansen M. The mystery of female connective tissue. Journal of Applied Physiology. 2008; 105(4):1026–1027. [PubMed: 18687974]

Kuo PL, Charng CC, Wu PC, Li PC. Shear-wave elasticity measurements of three-dimensional cell cultures for mechanobiology. Journal of Cell Science. 2017; 130(1):292–302. [PubMed: 27505887]

Li X, Wang JN, Fan ZY, Kang S, Liu YJ, Zhang YX, Wang XM. Determination of the elasticity of breast tissue during the menstrual cycle using real-time shear wave elastography. Ultrasound in Medicine & Biology. 2015; 52(12):3140–3147.

Loupas T, Gill RW, Peterson RB. Experimental evaluation of velocity and power estimation for ultrasound blood flow imaging, by means of a two-dimensional autocorrelation approach. IEEE Transactions on Ultrasonics, Ferroelectrics, and Frequency Control. 1995; 42(4):689–699.

Muller M, Aït-Belkacem D, Hessabi M, Gennisson JL, Grangé G, Goffinet F, Lecarpentier E, Cabrol D, Tanter M, Tsatsaris V. Assessment of the cervix in pregnant women using shear wave elastography: A feasibility study. Ultrasound in Medicine & Biology. 2015; 41(11):2789–2797. [PubMed: 26278635]

Myers KM, Paskaleva AP, House M, Socrate S. Mechanical and biochemical properties of human cervical tissue. Acta Biomaterialia. 2008; 4(1):104–16. [PubMed: 17904431]

Namani R, Wood MD, Sakiyama-Elbert SE, Bayly PV. Anisotropic mechanical properties of magnetically aligned fibrin gels measured by magnetic resonance elastography. Journal of Biomechanics. 2009; 42:2047–2053. [PubMed: 19656516]

Nightingale K. Acoustic radiation force impulse (arfi) imaging: a review. Current Medical Imaging Reviews. 2011; 7(4):328–339. [PubMed: 22545033]

Nightingale K, Rouze N, Rosenzweig S, Wang M, Abdelmalek M, Guy C, Palmeri M. Derivation and analysis of viscoelastic properties in human liver: impact of frequency on fibrosis and steatosis staging. IEEE Transactions on Ultrasonics, Ferroelectrics, and Frequency Control. 2015; 62(1): 165–175.

Owiti GEO, Tarantal AF, Lasley BL, Hendrickx AG. The effect of the anti-progestin ru 486 on early pregnancy in the long-tailed macaque (macaca fascicularis). Contraception. 1989; 40(2):201–211. [PubMed: 2758841]

Palmeri ML, Wang MH, Dahl JJ, Frinkley KD, Nightingale KR. Quantifying hepatic shear modulus in vivo using acoustic radiation force. Ultrasound in Medicine & Biology. 2008; 34(4):546–558. [PubMed: 18222031]

Peralta L, Mourier E, Richard C, Charpigny G, Larcher T, Aït-Belkacem D, Balla NK, Brasselet S, Tanter M, Muller M, Chavatte-Palmer P. In vivo evaluation of cervical stiffness evolution during induced ripening using shear wave elastography, histology and 2 photon excitation microscopy: Insight from an animal model. PLoS ONE. 2015; 10(8):e0133377. [PubMed: 26317774]

Peralta L, Rus G, Bochud N, Molina FS. Mechanical assessment of cervical remodelling in pregnancy: Insight from a synthetic model. Journal of Biomechanics. 2015; 48(9):1557–1565. [PubMed: 25766389]

R Core Team. R: A language and environment for statistical computing. 2013. URL: http://www.R-project.org/

Reusch LM, Feltovich H, Carlson LC, Hall G, Campagnola PJ, Eliceiri KW, Hall TJ. Nonlinear optical microscopy and ultrasound imaging of human cervical structure. Journal of Biomedical Optics. 2013; 18(3):031110. [PubMed: 23412434]

Rosado-Mendez IM, Guerrero QW, Drehfal LC, Santoso AP, Subramanian S, Kohn S, Shotzko M, Palmeri ML, Feltovich H, Hall TJ. Changes in cervical stiffness during pregnancy: Preliminary assessment with shear wave elasticity imaging in the rhesus macaque. AIP Conference Proceedings. 2016; 1747:1–8. URL: http://doi.org/10.1063/1.4954109.

Rosado-Mendez IM, Palmeri ML, Drehfal LC, Guerrero QW, Simmons H, Feltovich H, Hall TJ. Assessment of structural heterogoeneity and viscosity in the cervix using shear wave elasticity imaging: Initial results from a rhesus macaque model. Ultrasound in Medicine & Biology. 2017; 43(4):790–803. [PubMed: 28189282]

Rouse DJ, Weiner SJ, Bloom SL, Varner MW, Spong CY, Ramin SM, Caritis SN, Grobman WA, Sorokin Y, Sciscione A, Carpenter MW, Mercer BM, Thorp JM, Malone FD, Harper M, Iams JD, Anderson GD. Failed labor induction. Obstetrics & Gynecology. 2011; 117(2):267–272. [PubMed: 21252738]

Rouze NC, Wang MH, Palmeri ML, Nightingale KR. Robust estimation of time-of-flight shear wave speed using a radon sum transformation. IEEE Transactions on Ultrasonics, Ferroelectrics, and Frequency Control. 2010; 57(12):21–24.

Sarvazyan A, Hall TJ, Urban MW, Fatemi M, Aglyamov SR, Garra BS. An overview of elastography - an emerging branch of medical imaging. Current Medical Imaging Reviews. 2011; 7(4):255–282. [PubMed: 22308105]

Spong CY, Berghella V, Wenstrom KD, Mercer BM, Saade GR. Preventing the first cesarean delivery. Obstetrics & Gynecology. 2012; 120(5):1181–1193. [PubMed: 23090537]

Swiatkowska-Freund M, Preis K. Cervical elastography during pregnancy: clinical perspectives. International Journal of Women's Health. 2017; 9:245–254.

Timmons BC, Reese J, Socrate S, Ehinger N, Paria BC, Milne GL, Akin ML, Auchus RJ, McIntire D, House M, Mahendroo M. Prostaglandins are essential for cervical ripening in lps-mediated preterm birth but not term or antiprogestin-driven preterm ripening. Endocrinology. 2014; 155(1): 287–298. [PubMed: 24189143]

Wang M, Byram B, Palmeri M, Rouze N, Nightingale K. On the precision of time-of-flight shear wave speed estimation in homogeneous soft solids: initial results using a matrix array transducer. IEEE Transactions on Ultrasonics, Ferroelectrics, and Frequency Control. 2013; 60(4):758–770.

Wang MH, Palmeri ML, Rotemberg VM, Rouze NC, Nightingale KR. Improving the robustness of time-of-flight based shear wave speed reconstruction methods using ransac in human liver in vivo. Ultrasound in Medicine & Biology. 2010; 36(5):802–813. [PubMed: 20381950]

Wolfgan MJ, Eisele SG, Knowles L, Browne MA, Schotzko ML, Golos T. Pregnancy and live birth from nonsurgical transfer of in vivo- and in vitro -produced blastocysts in the rhesus monkey. Journal of Medical Primatology. 2001; 30(3):148–155. [PubMed: 11515670]

Yao W, Gan Y, Myers KM, Vink JY, Wapner RJ, Hendon CP. Collagen fiber orientation and dispersion in the upper cervix of non-pregnant and pregnant women. PloS One. 2016; 11(11):e0166709. [PubMed: 27898677]

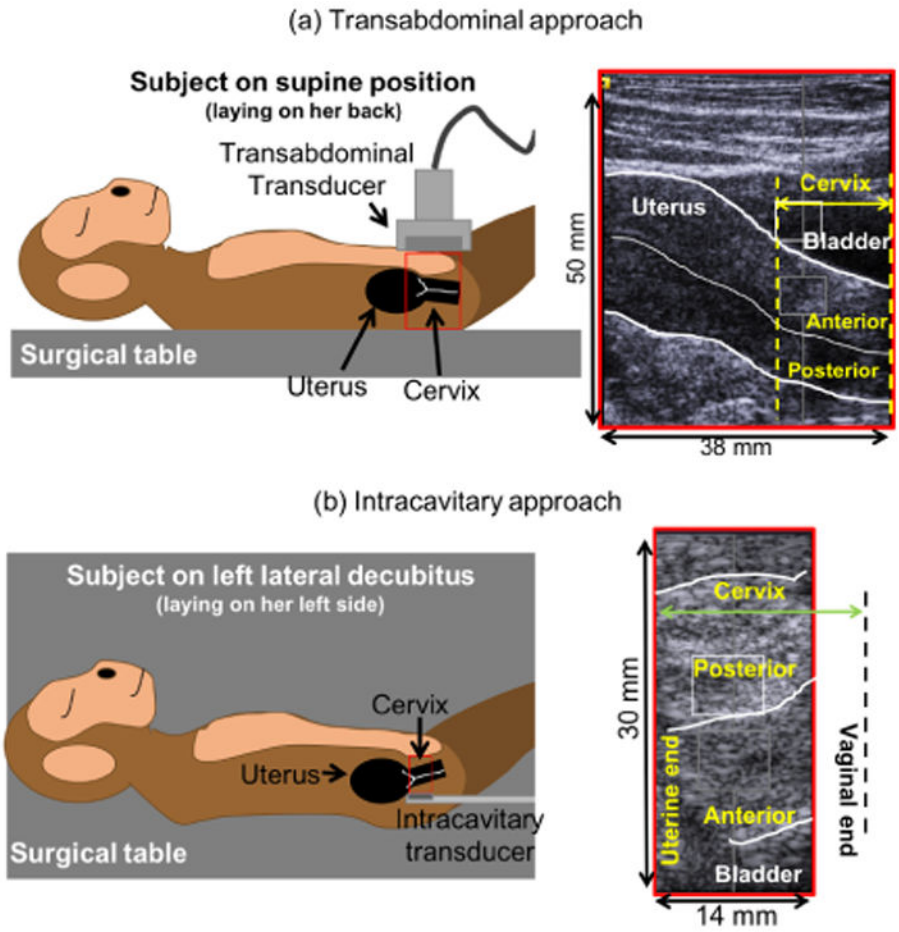

Figure 1.

Diagrams and B-mode images showing the position of the transducer in the transabdominal and intracavitary approaches and the anatomical landmarks. Leftside diagrams do not represent exact dimensions. Adapted from (Rosado-Mendez, Guerrero, Drehfal, Santoso, Subramanian, Kohn, Shotzko, Palmeri, Feltovich & Hall 2016), with the permission of AIP Publishing.

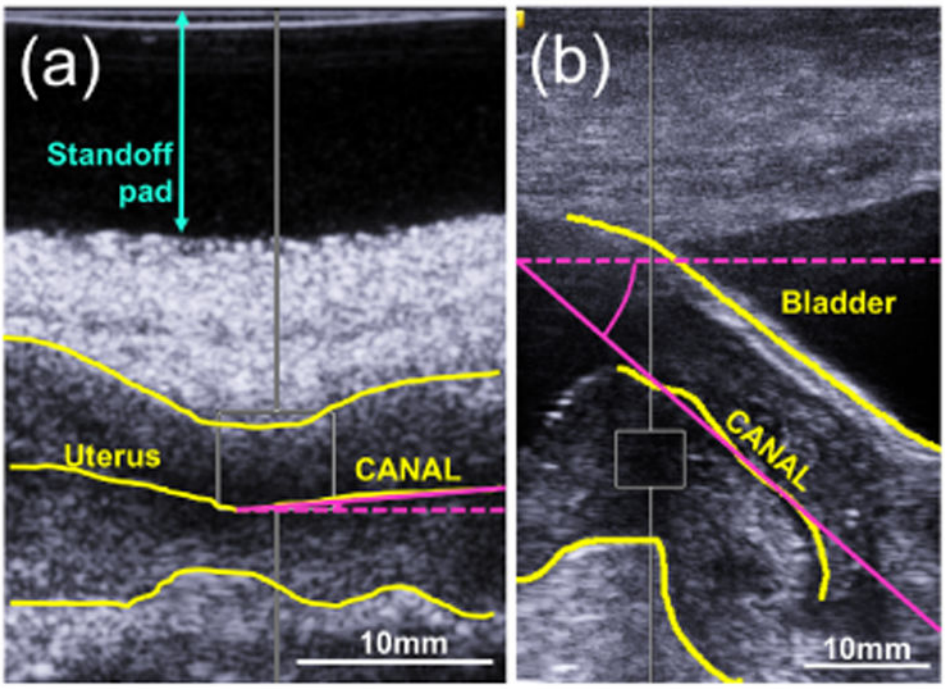

Figure 2.

Measurement of the angle between the cervical canal and the transducer aperture. Yellow lines indicate the anterior and posterior borders of the cervix and the cervical canal. Pink lines indicate the aperture over which the angle was measured. (a) 4.0° angle. (b) 41.6° angle.

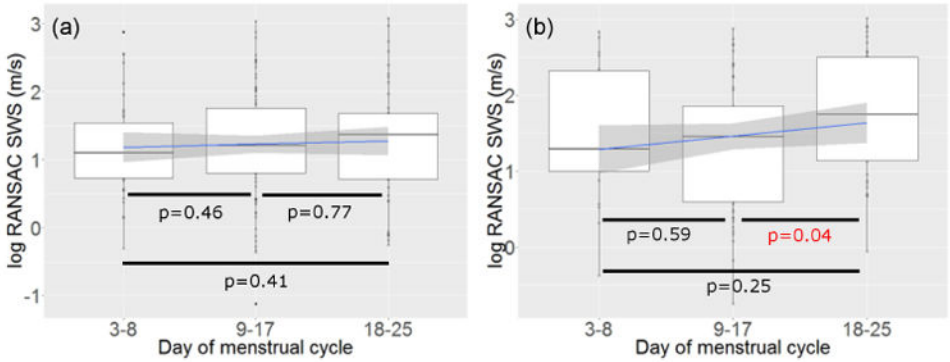

Figure 3.

SWS (log-transformed) vs. day within the menstrual cycle at the (a) anterior side and (b) posterior side. The blue line and shadowed area are the linear smoother and its 95% confidence interval. *p* values were obtained from the Kruskal-Wallis nonparametric test of statistical significance

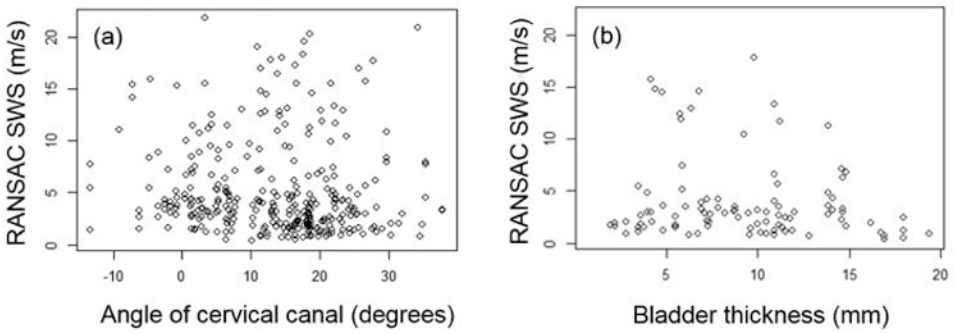

Figure 4.

SWS vs. (a) angle between the cervical canal and the transducer aperture and (b) thickness of the bladder in the axis between the transducer and the center of the ARFI ROI.

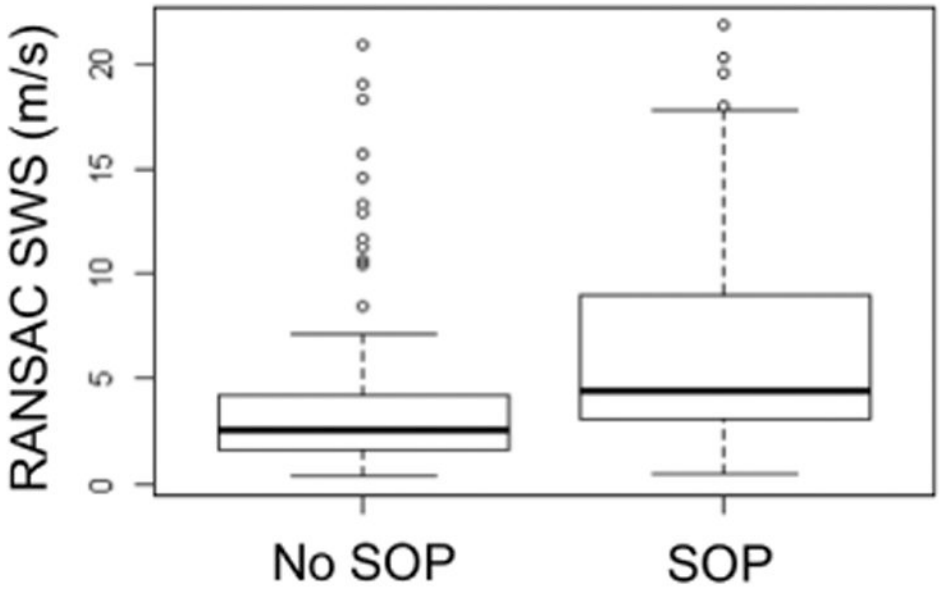

Figure 5.

Comparison of SWS estimates in the nonpregnant cervix when the standoff pad (SOP) was or was not used. Box plots indicate the median (middle line), the interquartile range (upper and lower limits), 1.5 times the interquartile range (whiskers), and outliers (circles).

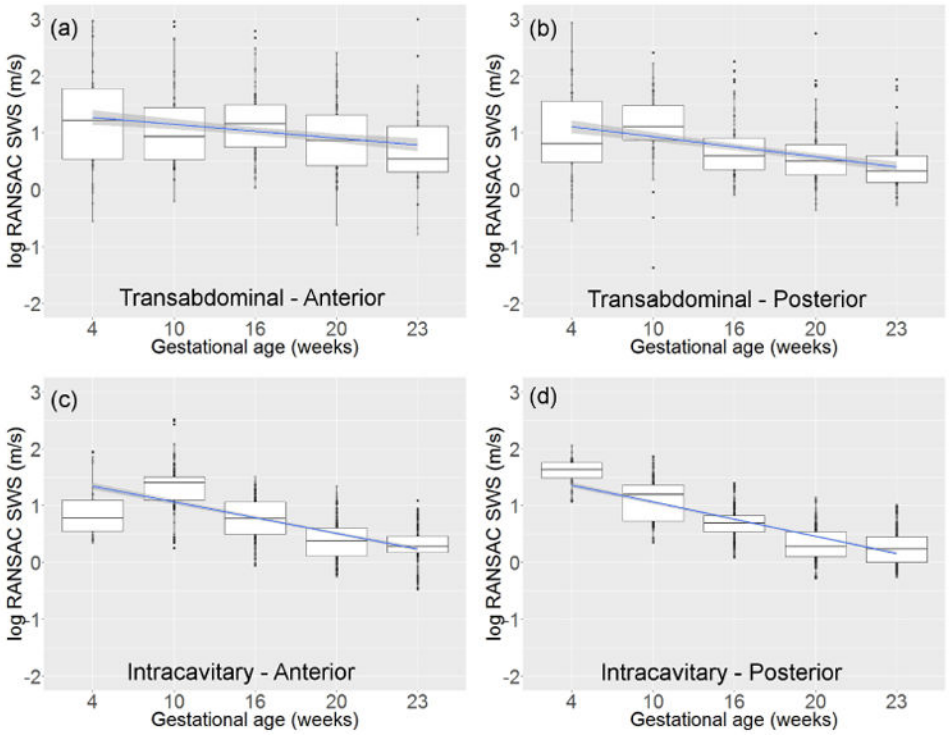

Figure 6.

SWS (log-transformed) vs. gestational age in weeks after conception for the transabdominal approach in (a) the anterior side and (b) the posterior side, and the intracavitary approach in (c) the anterior side and (b) the posterior side. The blue line and shadowed area are the linear smoother and its 95% confidence interval

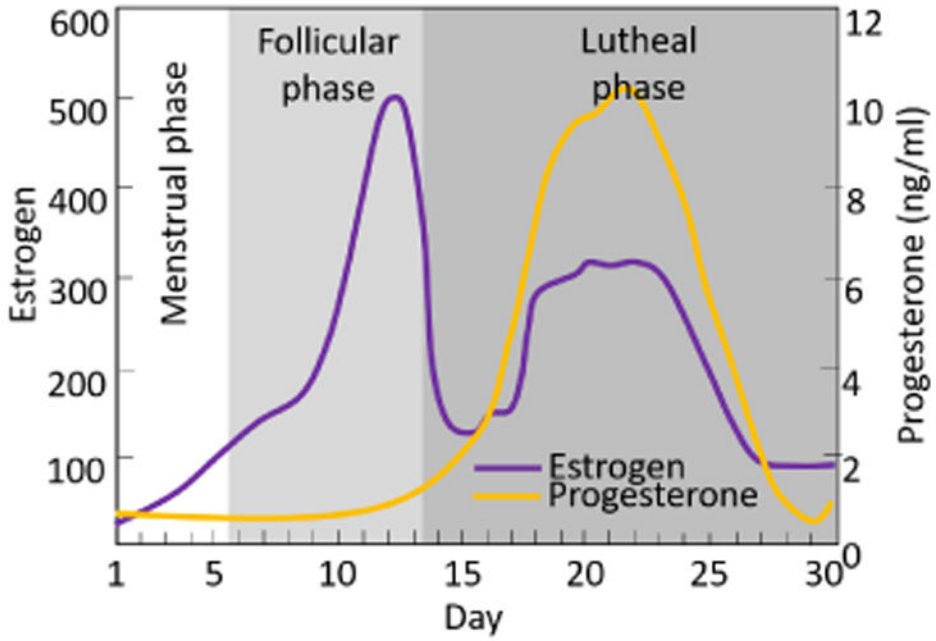

Figure 7. Changes in estrogen and progesterone levels during the menstrual cycle. Modified from Heitz et al. (Heitz, Eisenman, Beck & Walker 1999)

Table 1

Subject number, and median [range] of age and weight in the pre-pregnancy and pregnancy stages.

	Number of subjects	Age [y/o]	Weight [kg]
Non-pregnant, nulliparous	5	4.6 [4.3-5.8]	6.8 [6.5-8.3]
Non-pregnant, multiparous	5	14.8 [10.2-17]	8.1 [6.7-13.7]
Pregnant, nulliparous	10	4.3 [3.6-5.8]	6.8 [5.2-8.3]
Pregnant, multiparous	8	10.8 [5.2-17.0]	7.8 [6.7-10.2]

Table 2

Values of the ARFI data acquisition parameters for the transabdominal (TA) and intracavitary (IC) approaches. IQR= interquartile range. PRF= pulse repetition frequency.

Parameter	TA	IC
Probe	9L4	Prototype Catheter
Push freq. (MHz)	4.0	6.15
Track freq. (MHz)	6.2	7.27
Push cycles	800	800
Push duration (μs)	129	110
Track PRF (kHz)	10	10
Push f-number	1.5	1.0
Track f-number	2.0	1.5
Push focal depth (cm)		
median	3.1	0.9
IQR	2.7-3.6	0.6-1.2

Table 3

Parameters of the LME model for SWS vs. day in the menstrual cycle in the nonpregnant NHP cervix. ‘Int’=Intercept.

Variable	Fixed effect	Log value	Linear value	95% CI	*p*
a´	Int	0.94	2.56	1.67-3.89	—
b´	Day	0.02	1.02	1.00-1.03	0.07
c	Side	0.25	1.28	1.05-1.55	0.02
d	Dir	-0.05	0.95	0.79-1.14	0.58
e	Par	0.18	1.20	0.78-1.86	0.41

Table 4

Parameters of the LME model for SWS vs. weeks of gestation in the pregnant cervix

Variable	Fixed effect	Log value	Linear value	95% CI	*p*
h	Int	1.53	4.60	3.94-5.37	—
j	GA	-0.06	0.94	0.93-0.95	<0.0001
k	App	-0.25	0.78	0.70-0.86	<0.0001
l	Side	-0.07	0.93	0.89-0.96	0.0001
m	Dir	-0.05	0.96	0.92-0.99	0.014
n	Par	0.10	1.10	0.93-1.31	0.27
o	App*GA	0.03	1.03	1.03-1.04	<0.0001
p	App*Side	-0.20	0.82	0.76-0.88	<0.0001
q	App*Dir	0.12	1.13	1.06-1.21	0.0004
r	App*Par	0.03	1.03	0.96-1.11	0.43